Biophysical Chemistry 25 (1986) 191–200
Elsevier



BPC 01104

# DYNAMICS OF SUPERHELICAL DNA STUDIED BY PHOTON CORRELATION SPECTROSCOPY

Jörg LANGOWSKI [a], Ursula GIESEN [b] and Christina LEHMANN [b]

[a] *EMBL, c/o ILL, 156X, F-38042 Grenoble Cedex, France and* [b] *Abteilung Biophysikalische Chemie, MHH, D-3000 Hannover 61, F.R.G.*

Received 7th May 1986
Revised manuscript received 1st September 1986
Accepted 22nd September 1986

*Key words: DNA; Superhelix; Dynamic light scattering; Polymer flexibility; Rotational diffusion; Multiexponential decomposition*

We have conducted photon correlation spectroscopy (PCS) studies on the plasmid pUC8 (2717 bp) in order to elucidate the internal dynamics of this superhelical DNA. We confirm that the first-order autocorrelation function of the scattered light from pUC8 solutions can be separated into two distinct exponential decay components, as first shown by Lewis et al. (R. Lewis, J.H. Huang and P. Pecora, Macromolecules 18 (1985) 944). A thorough analysis of the dependence on scattering vector $\boldsymbol{K}$ of the rates and amplitudes of the two components enables us to assign the slowly relaxing part to the center-of-mass diffusion of the DNA, while the faster component corresponds to rotational, bending and twisting motions of the superhelix. For larger $\boldsymbol{K}$ values the internal motions can be formally expressed in terms of an 'internal diffusion coefficient' $D_i$, whose value of $2.0–2.5 \times 10^{-11}$ $m^2$ $s^{-1}$ is approximately equal to the translational diffusion coefficient predicted for a stiff DNA piece of the persistence length, 65 nm. Comparison of our measured $D_i$ values to those predicted from a recent theory of circular worm-like coils (K. Soda, Macromolecules 17 (1984) 2365) shows that the internal motions are faster than the theoretical values. One of the reasons for this discrepancy could be that the theory does not take into account torsional motions, which contribute significantly to the internal dynamics (J.C. Thomas, S.A. Allison, C.J. Appelof and J.M. Schurr, Biophys. Chem. 12 (1980) 177). At low $\boldsymbol{K}$ values, the fast relaxation rate of superhelical pUC8 is no longer proportional to $\boldsymbol{K}^2$, but reaches a constant value as $\boldsymbol{K}$ approaches zero. This behavior, not seen for the linearized DNA, can be interpreted in terms of rotational diffusion of a flexible rod-like molecule (T. Maeda and S. Fujime, Macromolecules 17 (1984) 2381) and supports an interwound rod-like structure for pUC8 DNA with an average end-to-end distance of 220 nm.

## 1. Introduction

The flexibility and internal motions of DNA have become a matter of considerable interest in recent years. It is by now an established fact that many biological processes which involve specific DNA-protein interactions are dependent not only on the primary base sequence of the DNA, but also on the conformational state of the double helix, and that this conformational state can vary depending on the environment [5–8]. Furthermore, the DNA structure – even in its 'normal' B-form – is flexible and fluctuates around its equilibrium position; studies of the physics of these motions will help to understand further DNA conformational changes and their role in regulation of genes, DNA packaging and chromatin structure.

A considerable amount of information on the bending flexibility of DNA has been obtained through studying the hydrodynamic conformation of linear DNA molecules in solution; from such experiments it is, e.g., rather straightforward to extract the persistence length of the DNA chain, which is related to the bending rigidity [9–11]. However, from these studies we obtain only information about the average static structure of the molecules; nothing is known about the dynamics

of the motion, its time scale and its molecular basis.

Many early studies on hydrodynamic properties of DNA used samples that were not very well defined, e.g., chicken erythrocyte DNA [12], and calf thymus DNA [13], often trimmed to a certain degree of monodispersity by controlled shearing or gel filtration [32]. Nowadays, studies in which the detailed dynamic behavior of DNA in solution is analyzed may be performed on better defined monodisperse samples, since it has become easy to prepare well defined DNA samples from plasmids that can be grown at high copy numbers, such as the pUC group of plasmids [14]. Additionally, with such DNAs the special structural features of superhelical DNA as compared to the linearized or open circular form can be easily studied.

One important method that has been used in recent years to measure internal motions in DNA and other flexible polymers is photon correlation spectroscopy (PCS), from which one obtains information about the Brownian motion of particles in solution by analyzing the intensity fluctuations of the scattered light [15,16].

In PCS studies on the dynamics of superhelical DNA it could, for instance, be shown that the large-scale motions of superhelical DNA and those of a short linear DNA fragment may be described by the same formalism after appropriate scaling [17]. Relaxation of superhelical DNA by *E. coli* single-strand binding protein leads to a significant increase in the internal motions [18]. A recent theory proposed by Soda [2] – an extension of an earlier model by Berg [2] – evaluated the Langevin equations for a circular chain made up of spherical beads, including hydrodynamic interactions. This model could be fitted to PCS data obtained on the ColE1 plasmid [33].

In those studies, the internal motions were mostly analyzed by either calculating the first cumulant (= initial slope of a semi-logarithmic plot) of the autocorrelation function or by force-fitting a single-exponential decay curve. From its relaxation time, an apparent diffusion coefficient $D_{app}$ may be calculated which equals the translational diffusion coefficient at small scattering vectors $\boldsymbol{K}$ and whose variation with $\boldsymbol{K}$ is characteristic of internal motions of the molecule (the term internal motions referring to all motions which are not purely translational, such as rotational diffusion, bending and torsion). The main reason for using only one parameter $D_{app}$ is that it is very hard to extract the times and amplitudes of multiple-exponential components from a noisy correlation spectrum and that very long data collection times on extremely dust-free samples are necessary to obtain spectra of sufficient quality for a more detailed analysis.

An earlier study by Caloin et al. [12] on calf thymus DNA samples showed that – at least in their case of a moderately polydisperse DNA preparation of very high molecular weight – two exponential decay components could be distinguished. Both relaxation rates were proportional to the square of the scattering vector $\boldsymbol{K}$ and could therefore be expressed as diffusion coefficients, the slower rate corresponding to translational diffusion of the whole DNA, the fast one corresponding, approximately, to the diffusion coefficient of the Rouse-Zimm subunit.

Recently, Lewis et al. [1] have analyzed the PCS of superhelical plasmid DNAs of different sizes. They showed the existence of discrete exponential components by applying the inverse Laplace transformation program CONTIN developed by Provencher [19]. Their study was performed at only two sets of scattering angles, one at 20–30° (with 488 nm light) yielding a single exponential corresponding to translational diffusion, and the other one 90°, where two discrete relaxation processes were seen, neither of which corresponded to the translational diffusion except for the smallest plasmid studied.

In the present paper we attempt to characterize the $\boldsymbol{K}$ dependence of the dynamic structure factor of superhelical and linearized plasmid DNA pUC8 (2717 base-pairs) in somewhat more detail, trying to connect the known behavior of bending rods and Gaussian coils in order to arrive at an empirical description of the autocorrelation function in the range $0 \leq \boldsymbol{K}L \leq 15$, where $L$ is the fully extended length of an interwound supercoiled structure.

## 2. Theory

The internal motions of a worm-like chain polymer can be related to PCS measurements by evaluation of the dynamic structure factor $S(\boldsymbol{K}, t)$ of the molecule [20]. Such a calculation is a formidable problem, because the Langevin equations for a worm-like filament with simultaneous bending, torsion and hydrodynamic interactions are intractable.

A number of approximative solutions to $S(\boldsymbol{K}, t)$ of a flexible polymer have been proposed: Lin and Schurr [13] derived an exact expression of the dynamic structure factor for the Rouse-Zimm model [30,31], and a later model by Berg [21], which was modified by Soda [2] to include hydrodynamic interactions, gave an approximate solution to the Langevin equation of a circular chain of adjacent spherical beads connected through a bending potential.

The Rouse-Zimm model successfully predicts the increase of the first cumulant diffusion coefficient with scattering vector as well as the plateau at high $\boldsymbol{K}$, and good agreement with experimental results on calf thymus DNA could be obtained [15]. Although the basis of the Rouse-Zimm model – a chain of globular subunits connected by stretching springs – is hard to relate to actual physical parameters of a worm-like chain, such as hydrodynamic radius, contour length and persistence length, it can nevertheless serve to compare the dynamics of different conformational states of DNA [18].

Single-exponential analysis of the autocorrelation function can only be approximative, because the contribution of internal motions to the autocorrelation function leads to additional faster decay terms [20], which make the autocorrelation function nonexponential [22]. Nevertheless, in this study we shall analyze our data as a sum of exponentials, trying to assign as many relaxation times as may reliably be extracted from the data. In order to obtain an idea of the validity of this approximation, let us examine the expression for the dynamic structure factor as it is obtained in the Berg-Soda theory [2,21,33]:

$$S(\boldsymbol{K}, t) \propto e^{-\boldsymbol{K}^2 D_0 t} \cdot \int_0^{L/2} \mathrm{d}s\, e^{-\left(\sum_{n=1}^{\infty} \frac{4kT\boldsymbol{K}^2}{3L\lambda_n}\left(1-\cos\left(\frac{2\pi n s}{L}\right)e^{-t/\tau n}\right)\right)} \quad (1)$$

where $\lambda_n$ are the eigenvalues of the solution of the Langevin equation of a closed circular chain of beads, $\tau_n$ the corresponding relaxation times and $L$ the contour length of the chain. In the low $\boldsymbol{K}^2$ limit when all eigenvalues but the first can be neglected, the integral can be evaluated:

$$S(\boldsymbol{K}, t) \propto e^{-\boldsymbol{K}^2 D_0 t} \cdot I_0\left(\frac{4kT\boldsymbol{K}^2}{3L\lambda_1} e^{-t/\tau_1}\right) \quad (2)$$

where $I_0(x)$ is the zero-order modified Bessel function of the first kind.

For small $\boldsymbol{K}^2$, eq. 2 simplifies to

$$S(\boldsymbol{K}, t) \approx e^{-\boldsymbol{K}^2 D_0 t} + \left(\frac{2kT\boldsymbol{K}^2}{3L\lambda_1}\right)^2 e^{-(\boldsymbol{K}^2 D_0 + 2/\tau_1)t} \quad (3)$$

It is apparent that in a range of sufficiently low $\boldsymbol{K}^2$ this model predicts that the first-order autocorrelation function will be a sum of two exponentials. The slower of the two decay times, inversely proportional to $\boldsymbol{K}^2$, will yield the translational diffusion coefficient, while the faster will in addition contain a $\boldsymbol{K}$-independent term that is related to the internal bending motion.

The limits of this approximation have been evaluated numerically in fig. 1. It is seen there that eq. 3 describes the exact numerical result from eq. 1 very well up to $\boldsymbol{K}^2 \approx 3 \times 10^{14}\ \mathrm{m}^{-2}$. Beyond that range, higher order terms would have to be included to account for the fact that $\tau_2$ stays approximately constant with $\boldsymbol{K}_2$; still, a double-exponential fit describes the data well.

There exist several other studies which evaluate theoretical expressions for the dynamic structure factor of weakly bending rods. From that work it is apparent that at low scattering vectors the biexponential decomposition is a valid approximation of the actual behavior of rigid and weakly bending rods as well.

The limiting value of the fast decaying component for $\boldsymbol{K} \to 0$ is then directly related to the rotational diffusion coefficient of the rod, as shown

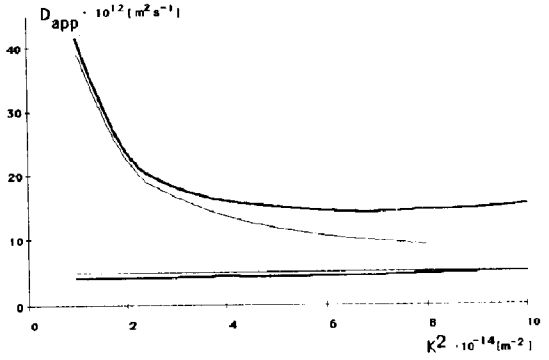


Fig. 1. Biexponential decomposition of the dynamic structure factor for a circular worm-like chain according to the Berg-Soda theory; relaxation rates are expressed as diffusion coefficients. Chain parameters were: contour length $L = 924$ nm, persistence length $a = 65$ nm, hydrodynamic radius $b = 1.25$ nm. Thick lines: fast (upper) and slow (lower) relaxations from a DISCRETE biexponential fit to eq. 1, which was numerically evaluated for the first five eigenvalues; thin lines, relaxation rates from the approximation, eq. 3.

for rigid rods in ref. 20 and recently for weakly bending rods by Maeda and Fujime [4].

Lewis et al. [1] used Pecora's model to describe their data [20], taking into account only rotational diffusion:

$$S(\boldsymbol{K}, t) \approx S_0(\boldsymbol{K}) e^{-\boldsymbol{K}^2 D_0 t} + S_1(\boldsymbol{K}) e^{-(\boldsymbol{K}^2 D_0 + 1/\tau_{rot})t} \tag{4}$$

The same basic result is obtained from Maeda and Fujime's description of the weakly bending rod [4].

$$S(\boldsymbol{K}, t) \approx S_0(\boldsymbol{K}) e^{-\boldsymbol{K}^2 D_0 t} + S_1(\boldsymbol{K}) e^{-(\boldsymbol{K}^2 D_0' + 1/\tau_{rot})} \tag{5}$$

where $D_0'$ in this case is composed of the translational diffusion coefficient $D_0$ and the two lateral diffusion coefficients $D_1$ and $D_3$, $D_0' = D_0 + (4/21)(D_3 - D_1)$.

One should note here that while the structure of eqs. 4 and 5 is very similar to that of eq. 3, the absolute value of the second relaxation time is quite different, as we will see later.

## 3. Materials and methods

### 3.1. Materials

pUC8 plasmid DNA was prepared from *E. coli* HB101 harboring the plasmid. Cells were lysed with lysozyme and detergent; crude DNA was obtained through RNAse/proteinase K treatment and several precipitation steps. Pure superhelical plasmid DNA was prepared by CsCl/ethidium density gradient centrifugation [18].

pUC8 DNA was linearized by incubation with restriction endonuclease *Eco*RI (Boehringer, Mannheim) in 0.1 M NaCl, 0.01 M Tris-HCl (pH 7.5), 0.02 M $MgCl_2$, checking for complete digestion by electrophoresis on 1% agarose gels. After digestion, the DNA solution was extracted with phenol to remove the enzyme, the plasmid precipitated with ethanol and redissolved in the buffer used for the light scattering experiment.

For PCS experiments, DNA solutions were prepared in 15 mm diameter cylindrical cuvettes. pUC8 was used at a concentration of 82 $\mu$g/ml in 0.1 M NaCl, 0.005 sodium phosphate (pH 7.0), 0.001 M EDTA. The DNA solution was filtered through a 0.4 $\mu$m Nuclepore polycarbonate filter. The filtration system was set up in such a way that any air entering the cuvette had to pass through a 0.2 $\mu$m Nucleopore filter, thereby minimizing dust contamination (M. Zulauf, personal communication). After experiments, DNA samples were checked for integrity by electrophoresis on 1% agarose gels. In no case was more than 10% of the superhelical DNA found in the nicked circular or linear form, neither could degradation of the linear DNA be detected.

### 3.2. Light scattering system

The light source used was a Spectra-Physics 166 $Ar^+$ ion laser operating at a wavelength of 488 nm at a power output of approx. 400 mW in light-regulation mode. Single longitudinal mode operation was assured by an intracavity Fabry-Perot etalon. The goniometer and observation optics were by AMTEC, Nice. The scattered light was collected by an EMI 9863 QB/100 photomultiplier, and the photon pulse train was analyzed by a Malvern

K7023 single-bit correlator with 88 channels and 4 delay channels. All measurements were done at ambient temperature (21–22°C); diffusion coefficients were temperature- and viscosity-corrected to $H_2O$ at 20°C.

For data analysis, autocorrelation functions were collected on an HP9825 calculator, which performed a preliminary double-exponential analysis. For later processing, the data sets were transferred to an Apple Macintosh computer or a VAX 11/750; programs there were in FORTRAN.

For each scattering vector, 8–10 separately collected autocorrelation functions (count rate $\approx 10^5$ $s^{-1}$, 4–6 min collection time) were accumulated using two different sampling times at each scattering vector. Only those measurements were used for the accumulation in which the relative difference between calculated total squared intensity (from the total count rate) and measured total squared intensity (from the delay channels) was less than 0.005. From the accumulated measurements, first-order autocorrelation functions were calculated using the relationship given in ref. 23:

$$G_1(\tau) = \text{sign}(G_2(\tau) - 1)\sqrt{|G_2(\tau) - 1|} \qquad (6)$$

A double-exponential analysis was done using the DISCRETE program developed by Provencher [24]. Some data sets were examined for the total number of individually distinguishable decay components using the CONTIN inverse Laplace transform program [19].

## 4. Results

### 4.1. Superhelical pUC8 DNA

In order to obtain a qualitative idea of the effect of internal motions on the diffusion coefficient of pUC8 measured in a dynamic light scattering experiment, we force-fitted a single-exponential decay curve to the intensity autocorrelation function and calculated 'apparent diffusion coefficients' $D_{app} = (2K^2\tau)^{-1}$ from their relaxation times $\tau$. Fig. 2 shows that $D_{app}$ increases with $K^2$; for small $K$, it extrapolates to the true translational diffusion coefficient $D_0$. In ref. 15 it had been shown that $D_{app}$ approaches a constant value at very high $K^2$, the level of which is determined by the extent of internal motions. This plateau could not be seen here due to the restricted range of $K$ available.

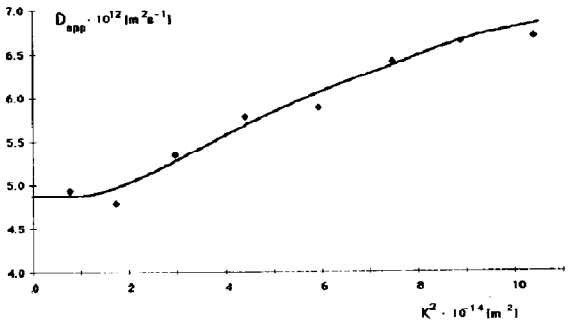


Fig. 2. Apparent diffusion coefficient of pUC8 plasmid DNA as a function of scattering vector. $D_{app}$ values were calculated from force-fitting a single exponential to a total decay of eight relaxation times.

Through the following multi-exponential analysis we could separate the contribution of internal motions from that of the translational diffusion. The DISCRETE program, developed to make plausible proposals with regard to the number of components contained in a multi-exponential decay function, yielded a double-exponential decay as the most probable fit to almost all our data (fig. 3). For consistency reasons, we always used the biexponential fit in our analysis.

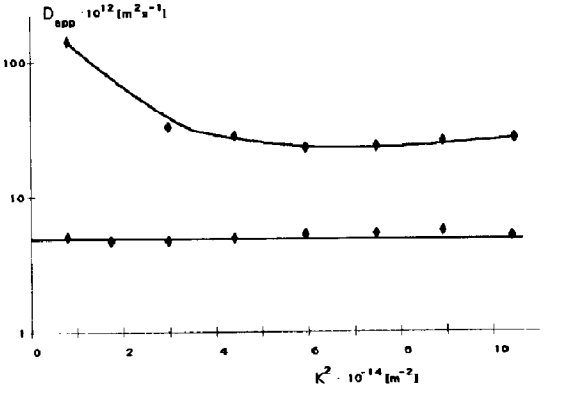


Fig. 3. Data from fig. 2 analyzed with the DISCRETE multiexponential fitting program. Lower curve, translational diffusion; upper curve, internal diffusion.

### 4.2. Inverse Laplace transform analysis; comparison with simulated data

In order to clarify whether the two exponential components proposed by the analysis were real or just a reflection of a continuous distribution of relaxation processes, we subjected some of the autocorrelation functions to the inverse-Laplace-transform analysis using the CONTIN program. Fig. 4 shows a typical result; it can be seen that the output actually predicts two peaks in the distribution function of exponential components, whose first moments are close to the discrete values from the double-exponential analysis.

For comparison, autocorrelation functions were simulated using the Berg-Soda model (eq. 1) and subjected to DISCRETE and CONTIN analyses. The only parameters required in eq. 1 are the contour length $L$, persistence length $a$ and hydrodynamic radius $b$ of the DNA. These values were set to $L = 924$ nm, $a = 65$ nm and $b = 1.25$ nm. Eq. 1 was numerically evaluated for the first five eigenvalues; inclusion of more eigenvalues did not change the result significantly in the $K^2$ range studied. Distribution functions obtained through inverse Laplace transformation of the simulated data show discrete peaks (fig. 5), and the most probable solution predicted from the discrete multicomponent analysis again is a biexponential (sometimes triexponential) decay curve in the range $K^2 = 2\text{–}10 \times 10^{14}$ m$^{-2}$. Although the analytical approximation (eq. 3) may be used only in the low-$K^2$ region, this result indicates that the solution of the BS model has a structure that

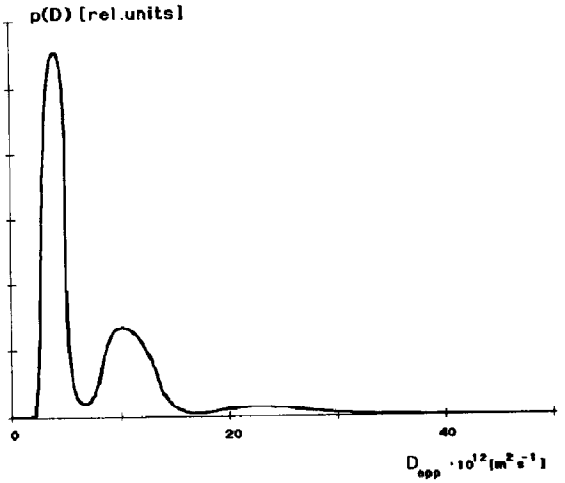


Fig. 5. Inverse Laplace transform of the dynamic structure factor of a circular worm-like chain for $K^2 = 9 \times 10^{14}$ m$^{-2}$ obtained through a CONTIN analysis of the numerical evaluation of the Berg-Soda model. Chain parameters as in fig. 1.

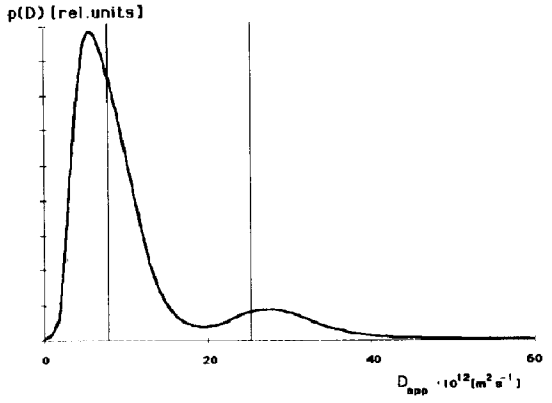


Fig. 4. Average multiexponential distribution of two data sets from fig. 2 at $K^2 = 10 \times 10^{14}$ m$^{-2}$, analyzed by the CONTIN inverse Laplace transform program in terms of a distribution function of apparent diffusion coefficients. Vertical lines indicate the result of the biexponential fit.

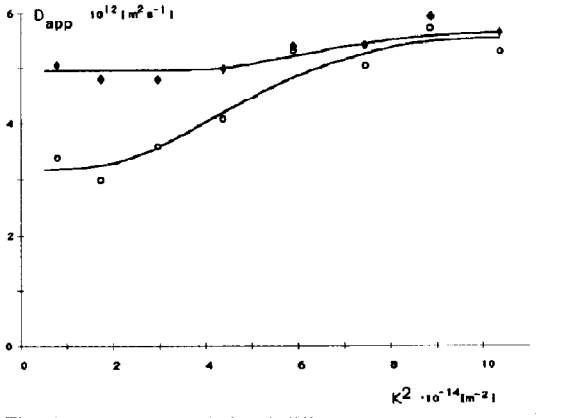


Fig. 6. Apparent translational diffusion coefficients (slow relaxation components) of superhelical (upper curve) and linear pUC8 (lower curve) as a function of scattering vector. Extrapolation to $K^2 = 0$ yields the true translational diffusion coefficients for both forms.

permits an analysis as a double-exponential decay at even higher $K^2$.

### 4.3. 'Diffusive' behavior of the internal motions

Both components of the biexponential decay can be expressed in terms of diffusion coefficients (fig. 3).

The slow-relaxing component $\tau_1$ yields a $K$-independent diffusion coefficient $D_t = (K^2\tau_1)^{-1}$ equal to the translational diffusion coefficient $D_0 = 4.9 \times 10^{-12}$ m$^2$ s$^{-1}$ obtained from fig. 2. The diffusion coefficient $D_i = (K^2\tau_2)^{-1}$, which is obtained from the fast-relaxing component, is approximately constant when $K^2 > 4 \times 10^{14}$ m$^{-2}$. For free superhelical and linear pUC8, the average value of $D_i$ in the range $K^2 = 4$–$10 \times 10^{14}$ m$^{-2}$ is around $2.5 \times 10^{-11}$ m$^2$ s$^{-1}$.

### 4.4. Low-K behavior and effect of linearization of the DNA

Fig. 6 compares the translational diffusion coefficients $D_t$ of superhelical and linearized pUC8. First we note that $D_t = 3.3 \times 10^{-12}$ m$^2$ s$^{-1}$ of the linear DNA is significantly smaller than that of the superhelical DNA, $D_t = 4.9 \times 10^{-12}$ m$^2$ s$^{-1}$. This is to be expected due to the more open structure of the linearized form. In fact, the diffusion coefficient obtained here is in good agreement with sedimentation studies on DNA fragments [9] as well as theoretical predictions by Yamakawa and Fuji [25]. The slow component of the linear DNA does not give a $K$-independent translational diffusion coefficient; the reason for this behavior could well be caused by the high amplitude of the fast component, which then precludes a good fit, creating artificially faster rates and higher amplitudes for the slow component. Whether or not a constant translational diffusion coefficient can adequately and consistently describe the data on linear DNA even at high $K^2$ is still an open question. A systematic extension of this study to superhelical and linear plasmid DNAs of different size and at different ionic strengths is underway and will eventually help to resolve this question.

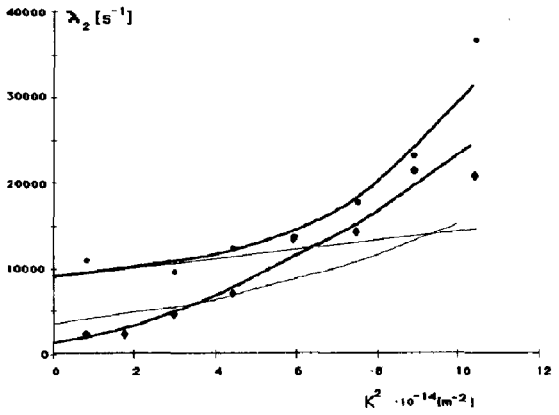


Fig. 7. Relaxation rates of the fast component for superhelical (upper thick line) and linear pUC8 (lower thick line) as a function of scattering vector. Lower thin line, Berg-Soda model; upper thin line, rotational relaxation only.

### 4.5. Internal motions of superhelical vs. linear DNA

The relaxation rates and amplitudes of the fast-relaxing component are plotted in figs. 7 and 8. The amplitude of the fast component of the linearized form is significantly higher than that of the superhelical form. Also, its amplitude increases very rapidly with $K$, while for the superhelical DNA this increase is much less pronounced. The leveling off of the curve for linear

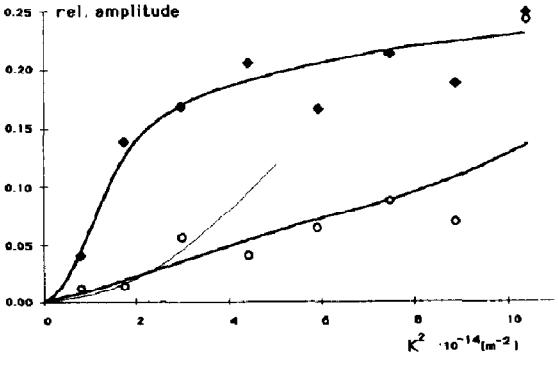


Fig. 8. Amplitudes of the fast-relaxing component for superhelical (lower line) and for linear pUC8 DNA (upper line) as a function of scattering vector. The theoretical behavior of the amplitude for the model chain used in fig. 1 is given by the thin line (in the approximation according to eq. 3).

DNA at higher $K$ could be due to the same reason as the previously mentioned increase of $D_t$ in this region.

## 5. Discussion

The apparent increase of the diffusion coefficient of superhelical pUC8 DNA with scattering vector $K$ is caused by fast-relaxing internal modes of motion of the DNA chain. These 'internal motions' may include: rotational relaxation of the whole molecule viewed as a rigid rod [4]; internal bending motions of the DNA chain [2,21] and torsional motions about the local helix axis [3]. Pure local torsional motions will not show up in a dynamic light scattering experiment, since by themselves they do not cause a redistribution of scattering density within the molecule; however, they may be coupled to bending deformations, thereby having indirect influence on the dynamic structure factor.

We could show in our experiments that the contribution of internal modes to the autocorrelation function can be described in good approximation by one fast single-exponential relaxation process in addition to the low relaxation caused by translational diffusion. The fast relaxation time, just as the slow one, is at high scattering vectors inversely proportional to $K^2$ and can therefore be described as an 'internal diffusion coefficient' $D_i$ in this regime. The increase of the apparent diffusion coefficient as obtained from the single-exponential analysis of the correlation function is due to an increasing amplitude of this fast internal relaxation.

A tentative explanation of a fast relaxation similar to that shown here has recently been given by Lewis et al. [1]. They subjected intensity scattering autocorrelation functions collected on various plasmid DNAs of defined size to an analysis by inverse Laplace transformation (CONTIN), obtaining two discrete relaxation processes very similar to those observed here. Since the fast relaxation was only shown for data collected at one angle (90°), it could not be shown conclusively whether the 'internal mode' observed was due to rotational diffusion or whether it could be described by a translational diffusion process. In the latter case, the observed internal diffusion coefficient should be independent of the scattering vector, while purely rotational diffusion gives rise to a biexponential decay with the slow component being the translational component, $\tau_1 = (K^2 D_t)^{-1}$, and the fast component containing in addition the rotational diffusion coefficient, $\tau_2 = (K^2 D_t + 6D_{rot})^{-1} = (K^2 D_i)^{-1}$. The same basic result is obtained using the more recent theory by Maeda and Fujime [4] (see above).

### 5.1. Structure of the pUC8 superhelix

Our results serve to unify the views of superhelical DNA as a rigid rod and as a locally bending filament. Rotational diffusion will only be detected if the molecule is anisotropic and contributes a $K$-independent term to the autocorrelation function. Therefore, our finding that the relaxation rate of the fast component remains nonzero at low $K$ indicates an overall anisotropic shape of the superhelix.

A fully extended interwound superhelical pUC8 would be 467 nm long, just half the contour length of the plasmid, and have an effective hydrodynamic diameter of (estimated) 3.5 nm, 1.4-times the hydrodynamic diameter of DNA. The rotational relaxation rate of such a rod would be [26] approx. 1000 $s^{-1}$. The rate of $10^4$ $s^{-1}$ that is measured here then would correspond to a length of 230 nm, assuming the hydrodynamic diameter stays more or less constant. From the difference of this length and the fully extended length we can draw some conclusions about the overall shape and flexibility of the superhelix in solution. (We assume in the following that the end-to-end distance of the proposed configuration determines the rotational relaxation rate, other configurational parameters being of minor influence).

Measurements by Brady and co-workers [27,28] as well as our own preliminary neutron scattering and magnetic birefringence data (J. Torbet and J. Langowski, unpublished data) suggest a distance of approx. 10 nm between opposing double strands and a pitch of 45° for the interwound form of the superhelix. Assuming this geometry, the end-to-end distance of a stiff interwound pUC8 would be

330 nm. The additional 30% 'shrinking' then reflects the average bending of the superhelix in solution; for uniform bending, the radius of curvature would be 120 nm.

*5.2. Internal motions of superhelical and linear pUC8.*

Above $K^2 = 4 \times 10^{14}$ m$^{-2}$, the experimental $D_i$ are significantly higher than the values predicted from the Berg-Soda model, the average in this range being $2.5 \times 10^{-11}$ m$^2$ s$^{-1}$ (fig. 3), while the theoretical value is $1.5 \times 10^{-11}$ m$^2 \cdot$ s$^{-1}$ (fig. 1). As fig. 7 shows, pure rotational diffusion cannot account for our observed relaxation rates either, since the increase of the fast relaxation time with $K^2$ is much faster than for rotational relaxation alone.

The discrepancy between out data and both models discussed indicates that the internal motion of superhelical DNA is not adequately described by a theory that takes into account only bending motions; neither can a superhelical DNA of this size be regarded as a riding rod, its only internal motion being rotational relaxation. Rather, there must exist additional processes that contribute faster components to the internal motions. It is obvious that torsion around the local helix axis, neglected in ref. 2, could be such a process. From other work [3] it is known that torsional motions in DNA occur on a nanosecond time scale. Torsional motions around the local helix axis by themselves will not give rise to fluctuations of polarizability in the DNA coil (on the length scale relevant here) and therefore do not influence the dynamic structure factor. However, torsional deformations can move parts of the DNA that are bent locally; through this coupling one can have additional contributions to the internal fluctuations that are faster than bending alone and therefore explain our discrepancy with Soda's theory.

The highly increased amplitudes of the fast relaxation in linear DNA compared to the superhelix reflect the open structure of the Gaussian coil, where the subparts of the chain are less restricted in their motion. However, the internal diffusion coefficients in the high $K$ region are very similar for linear and superhelical DNA (as seen from the slopes of the curves at high $K$ in fig. 7), indicating that the size of the independently moving subunit remains unchanged. It is interesting to note that $D_i$ is equal to the diffusion coefficient of a stiff linear DNA piece of the order of the persistence length [29] (or approx. 2 persistence lengths of a flexible DNA piece), which suggests that one could be able to describe DNA internal motions by a model in which individual segments of this length move more or less independently. This would allow a new way of extraction of a persistence-length-dependent parameter, namely $D_i$, from dynamic scattering experiments, in addition to the known methods of determining persistence lengths from length dependence of sedimentation or diffusion coefficients. We are currently investigating the feasibility of such a model by studying the dependence of $D_i$ on the contour length of the DNA.

Recently we obtained evidence that in a biological polymer of a completely different group – the porcine submaxillary mucin – a very similar internal diffusion process describes the internal motion (Giesen et al., in preparation).

## Acknowledgments

We thank Mickey Schurr and Bernard Jacrot for enlightening and helpful discussions. Part of the preliminary work for this paper was done on a light scattering system at the Institut für Biophysikalische Chemie in Hannover. We are grateful to Ekkehard Schuppe and his workshop for expert help in setting up that system. This work was supported by DFG grants La 500/3-1 and Heisenberg fellowship La 500/2-1 to J.L.

## References

1 R. Lewis, J.H. Huang and P. Pecora, Macromolecules 18 (1985) 944.
2 K. Soda, Macromolecules 17 (1984) 2365.
3 J.C. Thomas, S.A. Allison, C.J. Appellof and J.M. Schurr, Biophys. Chem. 12 (1980) 177.
4 T. Maeda and S. Fujime, Macromolecules 17 (1984) 2381.
5 F. Pohl and T.M. Jovin, J. Mol. Biol. 67 (1972) 375.
6 C.K. Singleton, J. Klysik, S.M. Stirdivant and R.D. Wells, Nature 299 (1982) 312.

7 D.M.J. Lilley, Nucleic Acids Res. 13 (1985) 1443.
8 I. Panyutin, V. Lyamichev and S. Mirkin, J. Biomol. Struct. Dyn. 2 (1985) 1221.
9 R.T. Kovacic and K.E. van Holde, Biochemistry 16 (1977) 1490.
10 J. Schellman, Biopolymers 13 (1974) 217.
11 Z. Kam, N. Borochov and H. Eisenberg, Biopolymers 20 (1981) 2671.
12 M. Caloin, B. Wilhelm and M. Daune, Biopolymers 16 (1977) 2091.
13 S.C. Lin and J.M. Schurr, Biopolymers 17 (1978) 425.
14 J. Vieira and J. Messing, Gene 19 (1982) 259.
15 J.M. Schurr, CRC Crit. Rev. Biochem. 4 (1977) 371.
16 J.M. Schurr, K.S. Schmitz, Annu. Rev. Phys. Chem. (1986) in the press.
17 J. Langowski, B.S. Fujimoto, D.E. Wemmer, A.S. Benight, G. Drobny, J.H. Shibata and J.M. Schurr, Biopolymers 24 (1985) 1023.
18 J. Langowski, A.S. Benight, B.S. Fujimoto and J.M. Schurr, Biochemistry 24 (1985) 4022.
19 S.W. Provencher, CONTIN V2 user's manual, EMBL technical report DA07, Heidelberg (1984).
20 B.J. Berne and R. Pecora, Dynamic light scattering (John Wiley, New York, 1976).
21 O.G. Berg, Biopolymers 18 (1979) 2861.
22 S.A. Aragon and R. Pecora, Macromolecules 18 (1985) 1868.
23 S.W. Provencher, Comp. Phys. Commun. 27 (1982) 229.
24 S.W. Provencher, Biophys. J. 16 (1976) 27.
25 H. Yamakawa and M. Fujii, Macromolecules 6 (1973) 407.
26 S. Broersma, J. Chem. Phys. 32 (1960) 1626.
27 G.W. Brady, D. Foos and C.J. Benham, Biopolymers 23 (1984) 2963.
28 G.W. Brady, D.B. Fein, H. Lambertson, V. Grassian, D. Foos and C.J. Benham, Proc. Natl. Acad. Sci. USA 80 (1983) 741.
29 M.M. Tirado and J. Garcia de la Torre, J. Chem. Phys. 71 (1979) 2581.
30 P.E. Rouse, J. Chem. Phys. 21 (1953) 1272.
31 B.H. Zimm, J. Chem. Phys. 24 (1956) 269.
32 M.T. Record, C.P. Woodbury and R.B. Inman, Biopolymers 14 (1975) 393.
33 K. Soda and A. Wada, Biophys. Chem. 20 (1984) 185.